Author Manuscript

Author Manuscript

Author Manuscript

Author Manuscript

HHS Public Access

Author manuscript

J Phys Chem Lett. Author manuscript; available in PMC 2019 March 01.

Published in final edited form as:

J Phys Chem Lett. 2018 March 01; 9(5): 1133–1139. doi:10.1021/acs.jpclett.7b03312.

Highly Stable, Ultra-Small Polymer-Grafted Nanobins (usPGNs) with Stimuli-Responsive Capability

Bong Jin Hong[1,5], **Aysenur Iscen**[2], **Anthony J. Chipre**[1], **Mei Mei Li**[1], **One-Sun Lee**[6], **Joshua N. Leonard**[2,3,4,5], **George C. Schatz**[1,*], and **SonBinh T. Nguyen**[1,5,*]

[1]Department of Chemistry and International Institute for Nanotechnology, Northwestern University, 2145 Sheridan Road, Evanston, Illinois 60208

[2]Department of Chemical and Biological Engineering, Northwestern University, 2145 Sheridan Road, Evanston, Illinois 60208

[3]Center for Synthetic Biology, Northwestern University, 2145 Sheridan Road, Evanston, Illinois 60208

[4]Chemistry of Life Processes Institute, Northwestern University, 2145 Sheridan Road, Evanston, Illinois 60208

[5]Robert H. Lurie Comprehensive Cancer Center, Northwestern University, 2145 Sheridan Road, Evanston, Illinois 60208

[6]Qatar Environment and Energy Research Institute, Hamad Bin Khalifa University, P.O. Box 5825, Doha, Qatar

Abstract

Highly stable and stimuli/pH-responsive ultra-small polymer-grafted nanobins (usPGNs) have been developed by grafting a small amount (10 mol %) of short (4.3 kDa) cholesterol-terminated poly(acrylic acid) (Chol-PAA) into an ultra-small unilamellar vesicle (uSUV). The usPGNs are stable against fusion and aggregation over several weeks and exhibit over 10-fold enhanced cargo retention in biologically relevant media at pH 7.4 in comparison with the parent uSUV template. Coarse-grained molecular dynamics (CGMD) simulations confirm that the presence of the cholesterol moiety can greatly stabilize the lipid bilayer. They also show extended PAA chain conformations that can be interpreted as causing repulsion between colloidal particles, thus stabilizing them against fusion. Notably, CGMD predicted a clustering of the Chol-PAA chains on the lipid bilayer under acidic conditions due to intra- and interchain hydrogen bonding, leading to the destabilization of local membrane areas. This explains the experimental observation that usPGNs can be triggered to release a significant amount of cargo upon acidification to pH 5. These

*Corresponding Author: g-schatz@northwestern.edu and stn@northwestern.edu.

Author Contributions

All authors have given approval to the final version of the manuscript.

Notes

The authors declare no competing financial interests.

Supporting Information. (1) Descriptions of experimental procedures, DLS, cryo-TEM, and cargo-release data and photos for uSUVs and usPGNs, and CGMD calculation (PDF), and (2) four MD simulation movies (MPG). These materials are available free of charge on the ACS Publications website at DOI: 10.1021/.

Author Manuscript Author Manuscript Author Manuscript Author Manuscript

developments put the lipid-bilayer-embedded Chol-PAA in stark contrast to traditional poly(acrylic acid) systems where the molar mass (M_n) of the polymer chains must exceed 16.5 kDa to achieve stimuli-responsive conformation changes. They also distinguish the small usPGNs from the much-larger polymer-caged nanobin (PCN) platform where the Chol-PAA chains must be covalently crosslinked to engender stimuli-responsive behaviors.

Graphical Abstract

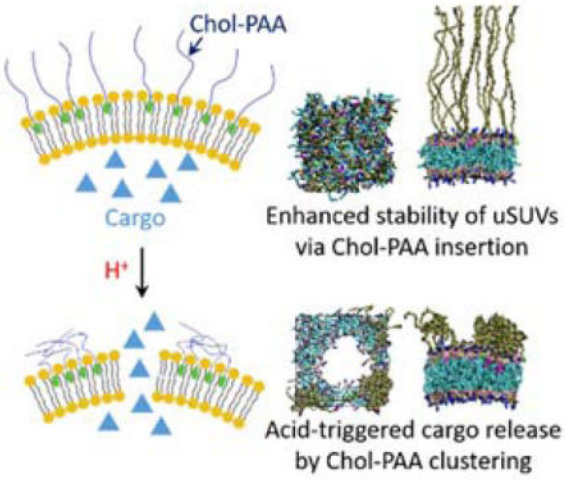

Keywords

ultra-small unilamellar vesicle; liposome; colloidal stability; lipid membrane stability; coarse-grained molecular dynamics (CGMD); stimuli-responsive polymer; polymer-grafted nanobin; smart delivery vehicle

---

Over the last decade, the utility of liposomal platforms in bio-nanotechnology has been greatly expanded through integration with a broad range of functional moieties, such as polymers, oligonucleotides, peptides, proteins, chelators, imaging agents, and small molecule drugs. Together with their excellent biocompatibility, easy accessibility, and tunable size distributions,[1–6] such functional incorporation has indeed enabled many promising applications in therapeutics,[1,6–8] diagnostics,[1,9–11] and assembly.[3–5] For example, the encapsulation of liposomal cores by stimuli-responsive polymer shells has transformed these highly biocompatible nanostructures into smart drug delivery platforms that can release bioactive payloads at a target site.[7] However, the relatively large sizes (hydrodynamic diameter (D_H) > 50 nm) of liposomes are still of concern for in vivo applications as they may result in poor particle penetration into target organs and tissues.[12–13] Indeed, particles in the 15–50 nm D_H range have been reported to be preferable for delivering therapeutics to hypovascularized cancers (e.g., pancreatic cancer),[13] mediating therapeutic transport across the blood-brain barrier,[14–15] carrying medicine transdermally,[16] and selectively targeting lymph nodes in vaccination.[17]

From a materials perspective, liposomes that are < 50 nm in diameter, henceforth referred to as ultra-small unilamellar vesicles (uSUVs),[18] are quite challenging to handle given their

Author Manuscript Author Manuscript Author Manuscript Author Manuscript

poor colloidal stability.[19–21] The highly strained, acute membrane curvature of these uSUVs often leads to a loose, disordered packing of the lipid molecules in the bilayer,[22] which in turn facilitates payload leakage, inter-particle fusion, and lipid membrane aggregation.[19–20,23–24] While several steric[25] and electrostatic[8,24] modification strategies have been attempted to improve the colloidal stability of uSUVs, the results have not been satisfactory: long-term colloidal stability remains low in biological media and there is still significant payload leakage. Prompted by our recent success in using grafted oligonucleotides to electrostatically stabilize uSUVs,[8] we hypothesized that uSUVs can be similarly stabilized with negatively charged poly(acrylic acid) grafts.[26] Most importantly, such grafts should endow the uSUVs with a stimuli-responsive function that is essential for a smart delivery platform.

Herein, we report the successful synthesis of ultra-small polymer-grafted nanobins[27] (usPGNs), a family of stable, stimuli-responsive polymer-grafted uSUVs that undergo triggered payload release in response to pH changes. Grafting a small amount (10 mol %) of short (~4.3 kDa) cholesterol-terminated poly(acrylic acid) (Chol-PAA) chains onto the membranes of uSUVs, made from lipids with a broad range of phase transition temperatures, dramatically enhances their long-term colloidal and membrane stability in biologically relevant media (pH 7.4, 20 mM HEPES and 150 mM NaCl). The cholesterol moieties of the grafted Chol-PAA polymers greatly increase the stability of the lipid-bilayer membranes post-insertion, as verified by coarse-grained molecular dynamics (CGMD) simulations. CGMD modeling additionally supports the notion that electrostatic repulsion, generated by the negatively charged carboxylic acid moieties of the embedded Chol-PAA chains, may be responsible for preventing lipid membrane fusion and aggregation. Notably, the stable lipid bilayer membrane of usPGNs can readily be destabilized by the grafted Chol-PAA shell upon mild acidification (pH 5.0), allowing for the spontaneous release of encapsulated cargo. Such destabilization was shown by CGMD simulations to occur through an acid-induced clustering of Chol-PAA chains on the lipid bilayer. Together, these biophysical insights strongly advocate for the use of stimuli-responsive polymer grafts to convert uSUVs into a highly promising class of “smart” nanocarriers for many applications.

Enhanced colloidal and membrane stability of uSUVs via Chol-PAA polymer grafting

To evaluate the potential of Chol-PAA polymer grafts to stabilize a broad range of uSUVs, we synthesized these templates from three different lipids with a broad range of phase-transition temperatures (T_m’s): 1,2-dipalmitoyl-*sn*-glycero-3-phosphocholine (DPPC), 1,2-dimyristoyl-*sn*-glycero-3-phosphocholine (DMPC), and 1,2-dioleoyl-*sn*-glycero-3-phosphocholine (DOPC) (T_m = 41, 24, and −17 °C, respectively). As both DPPC and DMPC have T_m’s that are higher than rt (20–22 °C), their uSUVs formulations are known to be less stable below this temperature range [19–21] and thus can be stabilized the most by polymer grafting. In a typical experiment, uSUVs with a diameter of ~25 nm were prepared from each of the three lipids using a modification of a published protocol[23] (Supporting Information (SI), Section S2). The as-prepared uSUVs were then grafted with 10 mol % of Chol-PAA (M_n = 4,300 Da, DP = 50, dispersity ($Đ$) = 0.12) following our previously

Author Manuscript Author Manuscript Author Manuscript Author Manuscript

reported “drop-in” method (Figure 1a).[26] Consistent with successful polymer grafting, the D_H’s of the resulting usPGN increases by ~10 nm in comparison to those of the parent uSUVs; the zeta (ζ) potentials of the usPGN also become significantly more negative (−45 ± 3 mV). Cryo-transmission electron microscopy (cryo-TEM; SI, Figure S2) images show that Chol-PAA insertion does not perturb the spherical morphology of the parent liposomal nanoparticles. As controls, we also synthesized two non-charged PEGylated DPPC-uSUVs by adding the appropriate PEGylated lipid (PE-PEG_{2000} and PE-PEG_{3000})[28] into the DPPC-SUV synthesis.[29]

Consistent with our hypothesis, the D_H’s of our DPPC- and DMPC-derived usPGN formulations (DPPC-usPGN and DMPC-usPGN, respectively) remained constant upon being stored in HEPES-buffered saline (HBS, 20 mM HEPES, 150 mM NaCl, pH 7.4) at either 4 °C or rt for over one month after preparation (Figure 1b–d; SI, Figure S3), indicating excellent colloidal stability. In stark contrast, the corresponding parent DPPC- and DMPC-uSUVs readily degraded under the same conditions: large flocculants and aggregates were observed within a couple of days after preparation (Figure 1b–d; see also SI, Figure S3). This is consistent with previously reported observations,[19–20,23] and had been attributed to the fact that the high-curvature lipid bilayers in these uSUVs fuse more easily at temperatures ≤ the T_m’s of DPPC and DMPC, resulting in aggregation.

As hypothesized in the introduction to this paper, the dramatically enhanced colloidal stability of our DPPC- and DMPC-usPGNs may be a consequence of extensive charge-repulsive stabilizations similar to those existing in liposomal spherical nucleic acid (LSNA).[8] This is supported by the large negative shift in the ζ potential of the lipid nanoparticles (to −45 ± 3 mV from a virtually neutral −3 ± 3 mV) after Chol-PAA insertion, which makes the usPGLs repel each other and prevent their fusion and aggregation, as predicted by the Derjaguin-Landau-Verwey-Overbeek theory.[30] Also consistent with our hypothesis is the observation that PEGylation, which has commonly been used to colloidally stabilize nanoparticles,[31–32] did not completely prevent fusion and aggregation of the control non-charged PEGylated DPPC-uSUVs, as previously reported for particles with high-curvature lipid bilayers.[33] While slower to fuse compared to the parent uSUVs, these PEGylated formulations also increased in size after synthesis (SI, Table S1) with relatively rapid aggregation and visible flocculent formation (SI, Figure S6). Together, these observations suggest that electrostatic stabilization via post-synthesis Chol-PAA grafts is a much more effective strategy for achieving colloidal stability of uSUV than stabilization through PEGylation.

In addition to good colloidal stability, DPPC- and DMPC-usPGNs also showed much less cargo leakage than did unmodified DPPC- and DMPC-uSUVs. When being stored at 4 °C, a temperature that is below the T_m’s of both DPPC and DMPC, calcein-loaded DPPC- and DMPC-usPGNs exhibited <4% leakage over a one-month period. In contrast, the corresponding uSUVs displayed significant leakage (54 and 42% for DPPC- and DMPC-uSUVs, respectively; Figures 1e and 1f) under the same conditions. Presumably, cargo leakage from these uSUVs can be attributed to their tendencies to rupture, fuse, and aggregate at this low temperature.

Author Manuscript Author Manuscript Author Manuscript Author Manuscript

While DOPC-derived uSUVs are already quite stable at temperature > T_m (Figure 1d), the stabilizing effect afforded by the cholesterol moiety[19,24,34] in Chol-PAA grafting (Figure 2a) is still quite significant upon examinations of dispersity data. The DOPC-usPGN remained much more monodispersed over a month of storage at both 4 °C and rt in contrast to the DOPC-derived uSUVs (SI, Figure S4). In addition, the Chol-PAA grafts also greatly reduced calcein cargo leakage from DOPC-usPGN, with <5% cargo leakage over 1 month of storage at 4 °C in comparison to 30% of leakage for the parent uSUVs (Figure 1g). The leakage of calcein from the latter is likely due to its diffusion through membrane defects,[22] which are more abundant as liposome size decreases.

Destabilization of the lipid bilayer membrane of usPGNs under acidic conditions by short Chol-PAA polymers

As previously reported,[7,35] the carboxylic acid group of PAA chains are ionizable and can readily associate with water and ions. However, because the backbone of PAA homopolymers is not very hydrophobic or sterically bulky, its conformations do not significantly change with pH unless the polymer chain reaches a molar mass (M_n) that exceeds 16.5 kDa.[35] As such, stimuli-responsive applications often rely on either covalent crosslinking of PAA[36] or on using a combination of PAA and other polymers such as poly(ethylene oxide), poly(acrylamide), or poly(vinyl alcohol), either as a physical mixture or as block copolymers (Figure 2b).[37] Our early work on large (~100 nm) polymer-caged liposomes for drug delivery employed both of these strategies simultaneously and can effect pH-sensitive cargo release with a 10 mol % insertion of Chol-PAA chains that are as short as 2.5 kDa.[26] At this low level of insertion and short polymer chain length, covalent crosslinking is critical for the chemomechanical response as cargo release does not occur with the non-crosslinked PGN template.

For the much smaller (<50 nm) SUVs, we hypothesize that crosslinking of the PAA chains would not be necessary. The inserted Chol-PAA chains are laterally more mobile on the more-strained lipid bilayer, and can be easily clustered together upon acidification through intra- and interchain hydrogen bonding (Figure 2c).[7] Such a phenomenon would significantly destabilize the initial cholesterol-stabilized membrane to cause cargo release (Figure 2c and 2d), without the need for covalently cross-linking the PAA chains.[26] It is also completely distinct from the traditional non-responsive behaviors of low-MW PAA-containing systems[35] due to the anchoring of the cholesterol moiety in the lipid bilayers. In other words, the synergistic combination of the Chol moiety and the PAA chain in our usPGNs should simultaneously afford cholesterol-enhanced stability at neutral pH and a pH-sensitive triggered release under acidic conditions.

As DOPC-derived SUVs were the most stable among our three uSUV formulations, we selected them to evaluate the extent of membrane destabilization by Chol-PAA under acidification. DOPC-usPGNs loaded with sulforhodamine B dyes (DOPC-usPGN$_{Rh}$) were placed in acidic (pH = 5.0) and neutral (pH = 7.4) buffer solutions, respectively (See SI, Sections S2e and S6). The usPGN solutions were then incubated at 37 °C, and the amount of dye released from the DOPC-usPGN$_{Rh}$ was regularly monitored by fluorescence

Author Manuscript Author Manuscript Author Manuscript Author Manuscript

spectroscopy. As shown in Figure 2d, a significant amount (40%) of encapsulated dyes was released from the DOPC-usPGN$_{Rh}$ after 24 h of incubation at pH 5.0 in comparison to a modest (< 10%) dye leakage from the pH 7.4 control. These behaviors are in stark contrast to the corresponding unmodified DOPC-uSUV$_{Rh}$, which showed similarly large cargo leakages at both acidic and neutral pHs (SI, Figure S7). Together, these observations strongly support our initial hypothesis: while the Chol-PAA shell of the usPGNs greatly stabilize the lipid bilayer at neutral pH compared to the parent SUVs, it can undergo a significant physical change upon acidification, destabilizing the membrane and leading to cargo release.

Coarse-grained molecular dynamics (CGMD) model and simulations

To model the physical changes conferred by Chol-PAA grafts on DOPC-usPGNs as a function of pH, we carried out coarse-grained molecular dynamics (CGMD) simulations.[38] Our DOPC-usPGN model was constructed by randomly dispersing 10 mol % of Chol-PAA polymer chain (DP = 50) on one side of a DOPC-derived “flat” lipid bilayer membrane (Figure 3e). Qa (−1 charge) and P3 (0 charge) beads were employed to respectively represent the deprotonated and protonated[39] states of the acrylic acid (AA) moieties in the Chol-PAA chains (Figures 3a and 3b). Four different bead ratios (Qa/P3 = 100/0, 70/30, 30/70, and 0/100) were used in our simulations to systematically correlate the physical changes brought about by changing the amount of protonated AA monomers. As control, a pure DOPC lipid bilayer membrane model without Chol-PAA chains was also constructed. The total CGMD simulation time for each system was 200 ns with 20 fs time steps, which is commonly used with the MARTINI force field (see SI, Sections S7 and S8 for details).

As shown in Figure 4b, CGMD simulation results show a clear collapse of the Chol-PAA chains with all protonated AA repeating units (Qa/P3 = 0/100) onto the lipid membrane, leading to the formation of large clusters due to attraction between the P3 beads. In contrast, the Chol-PAA chains with all deprotonated AA repeating units (Qa/P3 = 100/0) extend away from the lipid bilayer and remain apart during the whole simulation due to intra- and inter-chain electrostatic repulsion between the negatively charged Qa beads (Figure 4a). The intermediate cases (Qa/P3 = 30/70 and 70/30) qualitatively follow this trend: the higher fraction of protonated AA moieties lead to more clustering of the Chol-PAA chains and “more collapsed” structure (Figure 4b; see also SI, Figure S10).

Strongly supporting our hypothesis, the clustering of Chol-PAA chains indeed brings their cholesterol anchors close together in the lipid bilayer, as shown by plots of the radial distribution functions (RDFs) (Figure 4c) for all four simulated DOPC lipid bilayers in our study. While all four plots show RDF peaks at ~ 1 and 2 nm, the peak at the shorter distance (1 nm) increases significantly as the fraction of protonated AA repeating units increases, indicating that more cholesterols were clustered together. Such clustering leads to a segregation of the lipid bilayer membrane into cholesterol-rich and -deficient areas at low pH and presumably would destabilize the membrane from the non-clustered configuration at neutral pH. This difference confirms that an acid-trigger release mechanism can indeed be engineered into our usPGN.

Author Manuscript Author Manuscript Author Manuscript Author Manuscript

While GCMD models of small liposomes (≤ 20 nm in size) have recently been reported,[22,40–41] such models are still too costly to implement for our usPGN (~ 35 nm) systems, where the inclusion of the Chol-PAA chains greatly increases the size of the model. As clustering of the Chol-PAA chains in our usPGN CGMD models could lead to membrane destabilization (see above), a more efficient strategy to evaluate their relative stabilities *in silico* is to subject all of them to a destabilizing condition, such as a negative lateral pressure, and evaluate the kinetics of rupture. Such a strategy has been applied to flat lipid bilayer models to simulate membrane destabilization and rupture of pure lipid membranes.[42–43] To this end, we subjected all four SUV and Chol-PAA-grafted DOPC membrane models to a range of destabilizing negative pressures (−25 to −50 bar) in the xy plane for an additional 40 ns after full equilibration (at 1 bar for 200 ns). Such negative pressures would stretch out the lipid bilayers laterally, eventually causing them to rupture with different kinetics. For our usPGN under such a scenario, membranes with more protonated AA moieties, which cause the Chol-PAA chains in the lipid bilayer to cluster more (see above), would lead to faster membrane ruptures.

During the allotted time (40 ns) in our CGMD simulations, a parent uSUV membrane model ruptures before any of the corresponding four usPGN membranes (SI, Figure S13). This result strongly supports our experimental data that the insertion of chol-PAA chains can greatly enhance the stability of the high-curvature lipid bilayer. However, as the lateral pressure becomes more negative, the Chol-PAA-grafted membranes with more protonated AA repeating units (P3 beads) become less stable and rupture faster (at −45 bar, membranes with Qa/P3 = 100/0, 70/30, 30/70, and 0/100 rupture at 15, 23, 27, and 37 s of simulation time, respectively; see Figure 4f). This membrane rupture trend was consistently observed up to −50 bar, with the rupture point occurring earlier at more negative lateral pressure (i.e., the rupture at −50 bar occurs at an earlier time point than that at −45 bar (SI, Figure S11)). Interestingly, the membrane rupture occurred in the cholesterol-deficient areas of the membrane in all of the simulations. Small, water-filled fissures were observed to form in these areas (SI, MD simulation movies), and these fissures quickly grew in size and merged into a large pore (Figure 4e), eventually causing complete membrane disassembly (SI, MD simulation movies). Together, these results from our CGMD simulations present a detailed picture of the mechanism by which Chol-PAA grafts can stabilize the lipid bilayer membrane of DOPC-usPGNs at neutral pH while facilitating cargo release under acidic environments.

In summary, we have demonstrated that low-level grafting of Chol-PAA polymers can endow colloidally unstable uSUVs with a negative ζ potential that enables them to remain dispersed in biologically relevant media for long periods. Additionally, these grafts can endow usPGNs with a combination of properties that are highly desirable for smart nanocarriers: remarkable cargo retention under physiologically relevant conditions and facile cargo release in response to acidification. As Chol-PAA grafting confers a large number of carboxyl moieties (~ 19,000/25 nm particle at 10 mol % modification) on the usPGN surface, this simple drop-in modification can extend the utility of uSUVs beyond the immediate benefits from their small sizes: the carboxyl groups can be used as a robust conjugation handle for other functional groups such as cellular-targeting ligands,[44] therapeutics,[45–46] and imaging agents.[10] Together, the desirable combination of high

Author Manuscript Author Manuscript Author Manuscript Author Manuscript

stabilities, triggered cargo release, and functionalization handles should enable usPGNs to be a robust and versatile scaffold for a highly promising class of smart nanocarriers for various applications. Fox example, the encapsulation of anticancer drugs such as doxorubicin[11] and gemcitabine[10] can allow these particles to be explored for targeted cancer therapy or theranostic.[10–11]

Supplementary Material

Refer to Web version on PubMed Central for supplementary material.

Acknowledgments

This work is financially supported by the NIH (NCI CCNE Grant U54CA199091, NCI CCNE Grant C54CA151880, CCNP Grant U01CA151461, and Core Grant P30CA060553 to the Lurie Cancer Center of Northwestern University (NU)). A. I. and G. C. S. were supported as part of the Center for Bio-Inspired Energy Science, an Energy Frontier Research Center funded by the U.S. Department of Energy, Office of Science, Basic Energy Sciences, under Award #DE-SC0000989-002. A. J. C was a fellow in the Molecular Biophysics Training Program at Northwestern University (NCI Grant T32GM008382). M. L. was supported by a Nanoscale Science and Engineering REU Program (NSF award number EEC-0647560) and a 2013–2014 academic year research grant from Northwestern University. J. N. L. additionally acknowledges supports from a 3M Nontenured Faculty Grant. Instruments in the Northwestern University IMSERC and Keck Biophysics facilities were purchased with grants from NSF-NSEC (NSF EEC–0647560), NIH-CCNE, NSF-MRSEC (NSF DMR-1121262), the Keck Foundation, the state of Illinois, and Northwestern University. The cryo-TEM work was carried out at the Structural Biology Facility at Northwestern University, which was partially supported by the R. H. Lurie Comprehensive Cancer Center. The Gatan K2 direct electron detector was purchased with funds provided by the Chicago Biomedical Consortium with support from the Searle Funds at The Chicago Community Trust.

References

1. Pattni BS, Chupin VV, Torchilin VP. New Developments in Liposomal Drug Delivery. Chem Rev. 2015; 115:10938–10966. [PubMed: 26010257]
2. Akbarzadeh A, Rezaei-Sadabady R, Davaran S, Joo SW, Zarghami N, Hanifehpour Y, Samiei M, Kouhi M, Nejati-Koshki K. Liposome: Classification, Preparation, and Applications. Nanoscale Res Lett. 2013; 8:1–9. [PubMed: 23279756]
3. Yang Y, Wang J, Shigematsu H, Xu W, Shih WM, Rothman JE, Lin C. Self-Assembly of Size-Controlled Liposomes on DNA Nanotemplates. Nat Chem. 2016; 8:476–483. [PubMed: 27102682]
4. Dave N, Liu J. Programmable Assembly of DNA-Functionalized Liposomes by DNA. ACS Nano. 2011; 5:1304–1312. [PubMed: 21230009]
5. Ma M, Bong D. Controlled Fusion of Synthetic Lipid Membrane Vesicles. Acc Chem Res. 2013; 46:2988–2997. [PubMed: 23879805]
6. Radovic-Moreno AF, Chernyak N, Mader CC, Nallagatla S, Kang RS, Hao L, Walker DA, Halo TL, Merkel TJ, Rische CH, Anantatmula S, Burkhart M, Mirkin CA, Gryaznov SM. Immunomodulatory Spherical Nucleic Acids. Proc Natl Acad Sci U S A. 2015; 112:3892–3897. [PubMed: 25775582]
7. Lee SM, Nguyen ST. Smart Nanoscale Drug Delivery Platforms from Stimuli-Responsive Polymers and Liposomes. Macromolecules. 2013; 46:9169–9180. [PubMed: 28804160]
8. Banga RJ, Chernyak N, Narayan SP, Nguyen ST, Mirkin CA. Liposomal Spherical Nucleic Acids. J Am Chem Soc. 2014; 136:9866–9869. [PubMed: 24983505]
9. Silindir M, Erdoğan S, Özer AY, Maia S. Liposomes and Their Applications in Molecular Imaging. J Drug Targeting. 2012; 20:401–415.
10. Lee SM, Song Y, Hong BJ, MacRenaris KW, Mastarone DJ, O'Halloran TV, Meade TJ, Nguyen ST. Modular Polymer-Caged Nanobins as a Theranostic Platform with Enhanced Magnetic Resonance Relaxivity and pH-Responsive Drug Release. Angew Chem, Int Ed. 2010; 49:9960–9964.
11. Hong BJ, Swindell EP, MacRenaris KW, Hankins PL, Chipre AJ, Mastarone DJ, Ahn RW, Meade TJ, O'Halloran TV, Nguyen ST. pH-Responsive Theranostic Polymer-Caged Nanobins: Enhanced

Author Manuscript Author Manuscript Author Manuscript Author Manuscript

Cytotoxicity and T1 MRI Contrast by Her2 Targeting. Part Part Syst Charact. 2013; 30:770–774. [PubMed: 24516291]

12. Tang L, Yang X, Yin Q, Cai K, Wang H, Chaudhury I, Yao C, Zhou Q, Kwon M, Hartman JA, Dobrucki IT, Dobrucki LW, Borst LB, Lezmi S, Helferich WG, Ferguson AL, Fan TM, Cheng J. Investigating the Optimal Size of Anticancer Nanomedicine. Proc Natl Acad Sci U S A. 2014; 111:15344–15349. [PubMed: 25316794]
13. Cabral H, Matsumoto Y, Mizuno K, Chen Q, Murakami M, Kimura M, Terada Y, Kano MR, Miyazono K, Uesaka M, Nishiyama N, Kataoka K. Accumulation of Sub-100 nm Polymeric Micelles in Poorly Permeable Tumours Depends on Size. Nat Nanotechnol. 2011; 6:815–823. [PubMed: 22020122]
14. Fresta M, Wehrli E, Puglisi G. Enhanced Therapeutic Effect of Cytidine-5′-Diphosphate Choline When Associated with G(M1) Containing Small Liposomes as Demonstrated in a Rat Ischemia Model. Pharm Res. 1995; 12:1769–1774. [PubMed: 8592684]
15. Betzer O, Shilo M, Opochinsky R, Barnoy E, Motiei M, Okun E, Yadid G, Popovtzer R. The Effect of Nanoparticle Size on the Ability to Cross the Blood–Brain Barrier: an In Vivo Study. Nanomedicine. 2017; 12:1533–1546. [PubMed: 28621578]
16. Sonavane G, Tomoda K, Sano A, Ohshima H, Terada H, Makino K. In Vitro Permeation of Gold Nanoparticles through Rat Skin and Rat Intestine: Effect of Particle Size. Colloids Surf, B. 2008; 65:1–10.
17. Reddy ST, van der Vlies AJ, Simeoni E, Angeli V, Randolph GJ, O'Neill CP, Lee LK, Swartz MA, Hubbell JA. Exploiting Lymphatic Transport and Complement Activation in Nanoparticle Vaccines. Nat Biotechnol. 2007; 25:1159–1164. [PubMed: 17873867]
18. Liposomes in the 20–100 nm range are traditionally called small unilamellar vehicle (SUV see Chem Rev. 2015; 115:10938–10966. [PubMed: 26010257]). In this work, we use the term "ultra-small unilamellar vehicle (uSUV)" to describe an SUV with $D_H \leq 50$ nm.
19. McConnell DS, Schullery SE. Phospholipid Vesicle Fusion and Drug Loading - Temperature, Solute and Cholesterol Effects, and, a Rapid Preparation for Solute-Loaded Vesicles. Biochim Biophys Acta. 1985; 818:13–22.
20. Schullery SE, Schmidt CF, Felgner P, Tillack TW, Thompson TE. Fusion of Dipalmitoylphosphatidylcholine Vesicles. Biochemistry. 1980; 19:3919–3923. [PubMed: 6893276]
21. Lentz BR, Carpenter TJ, Alford DR. Spontaneous Fusion of Phosphatidylcholine Small Unilamellar Vesicles in the Fluid Phase. Biochemistry. 1987; 26:5389–5397. [PubMed: 3676258]
22. Lin CM, Li CS, Sheng YJ, Wu DT, Tsao HK. Size-Dependent Properties of Small Unilamellar Vesicles Formed by Model Lipids. Langmuir. 2012; 28:689–700. [PubMed: 22126796]
23. Wong M, Anthony FH, Tillack TW, Thompson TE. Fusion of Dipalmitoylphosphatidylcholine Vesicles at 4 °C. Biochemistry. 1982; 21:4126–4132. [PubMed: 6896998]
24. Mercadal M, Domingo JC, Bermudez M, Mora M, Demadariaga MA. N-Palmitoylphosphatidylethanolamine Stabilizes Liposomes in the Presence of Human Serum - Effect of Lipidic Composition and System Characterization. Biochim Biophys Acta. 1995; 1235:281–288. [PubMed: 7756336]
25. Savarala S, Ahmed S, Ilies MA, Wunder SL. Stabilization of Soft Lipid Colloids: Competing Effects of Nanoparticle Decoration and Supported Lipid Bilayer Formation. ACS Nano. 2011; 5:2619–2628. [PubMed: 21381770]
26. Lee SM, Chen H, Dettmer CM, O'Halloran TV, Nguyen ST. Polymer-Caged Lipsomes: A pH-Responsive Delivery System with High Stability. J Am Chem Soc. 2007; 129:15096–15097. [PubMed: 17999499]
27. The term nanobin was originally coined to indicate the broad range of cargos that can be loaded into these polymer-caged nanocarriers (see J Am Chem Soc. 2009; 131:9311–9320. [PubMed: 19527027]
28. PE = 1,2-dimyristoyl-sn-glycero-3-phosphoethanolamine. The subscript number following the PEG notation indicates the molecular weight of the PEG chain.
29. This simple PEGylation protocol has been commonly employed in the synthesis of stealth liposome, such as Doxil™to improve stabilization and engender in vivo stealth capabilities and

Author Manuscript Author Manuscript Author Manuscript Author Manuscript

longer circulation (see Int J Nanomed. 2006; 1:297–315. and Curr Drug Metab. 2012; 13:105–119. [PubMed: 21892917]

30. Laaksonen T, Ahonen P, Johans C, Kontturi K. Stability and Electrostatics of Mercaptoundecanoic Acid-Capped Gold Nanoparticles with Varying Counterion Size. ChemPhysChem. 2006; 7:2143–2149. [PubMed: 16969881]
31. Torchilin VP. Recent Advances with Liposomes as Pharmaceutical Carriers. Nat Rev Drug Discovery. 2005; 4:145–160. [PubMed: 15688077]
32. Suk JS, Xu Q, Kim N, Hanes J, Ensign LM. PEGylation as a Strategy for Improving Nanoparticle-Based Drug and Gene Delivery. Adv Drug Delivery Rev. 2016; 99:28–51.
33. Evans KO, Lentz BR. Kinetics of Lipid Rearrangements during Poly(ethylene Glycol)-Mediated Fusion of Highly Curved Unilamellar Vesicles. Biochemistry. 2002; 41:1241–1249. [PubMed: 11802723]
34. Roy SM, Bansode AS, Sarkar M. Effect of Increase in Orientational Order of Lipid Chains and Head Group Spacing on Non Steroidal Anti-Inflammatory Drug Induced Membrane Fusion. Langmuir. 2010; 26:18967–18975. [PubMed: 21114267]
35. Swift T, Swanson L, Geoghegan M, Rimmer S. The pH-Responsive Behaviour of Poly(acrylic Acid) in Aqueous Solution is Dependent on Molar Mass. Soft Matter. 2016; 12:2542–2549. [PubMed: 26822456]
36. Elliott JE, Macdonald M, Nie J, Bowman CN. Structure and Swelling of Poly(acrylic Acid) Hydrogels: Effect of pH, Ionic Strength, and Dilution on the Crosslinked Polymer Structure. Polymer. 2004; 45:1503–1510.
37. Huynh CT, Nguyen MK, Lee DS. Injectable Block Copolymer Hydrogels: Achievements and Future Challenges for Biomedical Applications. Macromolecules. 2011; 44:6629–6636.
38. Marrink SJ, Risselada HJ, Yefimov S, Tieleman DP, de Vries AH. The MARTINI Force Field: Coarse Grained Model for Biomolecular Simulations. J Phys Chem B. 2007; 111:7812–7824. [PubMed: 17569554]
39. As P3 beads have been used to represent acetic acids and their interaction in solution (see J Phys Chem B. 2007; 111:7812–7824. [PubMed: 17569554]), we feel that it can describe the acrylic acid moieties in our polymers well.
40. Risselada HJ, Marrink SJ. Curvature Effects on Lipid Packing and Dynamics in Liposomes Revealed by Coarse Grained Molecular Dynamics Simulations. Phys Chem Chem Phys. 2009; 11:2056–2067. [PubMed: 19280016]
41. Louhivuori M, Risselada HJ, van der Giessen E, Marrink SJ. Release of Content through Mechano-Sensitive Gates in Pressurized Liposomes. Proc Natl Acad Sci U S A. 2010; 107:19856–19860. [PubMed: 21041677]
42. Xie JY, Ding GH, Karttunen M. Molecular Dynamics Simulations of Lipid Membranes with Lateral Force: Rupture and Dynamic Properties. Biochim Biophys Acta, Biomembr. 2014; 1838:994–1002.
43. Leontiadou H, Mark AE, Marrink SJ. Molecular Dynamics Simulations of Hydrophilic Pores in Lipid Bilayers. Biophys J. 2004; 86:2156–2164. [PubMed: 15041656]
44. Lee SM, Chen HM, O'Halloran TV, Nguyen ST. "Clickable" Polymer-Caged Nanobins as a Modular Drug Delivery Platform. J Am Chem Soc. 2009; 131:9311–9320. [PubMed: 19527027]
45. Lee SM, O'Halloran TV, Nguyen ST. Polymer-Caged Nanobins for Synergistic Cisplatin-Doxorubicin Combination Chemotherapy. J Am Chem Soc. 2010; 132:17130–17138. [PubMed: 21077673]
46. Lee SM, Lee OS, O'Halloran TV, Schatz GC, Nguyen ST. Triggered Release of Pharmacophores from [Ni($HAsO_3$)]-Loaded Polymer-Caged Nanobin Enhances Pro-apoptotic Activity: A Combined Experimental and Theoretical Study. ACS Nano. 2011; 5:3961–3969. [PubMed: 21466214]

Author Manuscript Author Manuscript Author Manuscript Author Manuscript

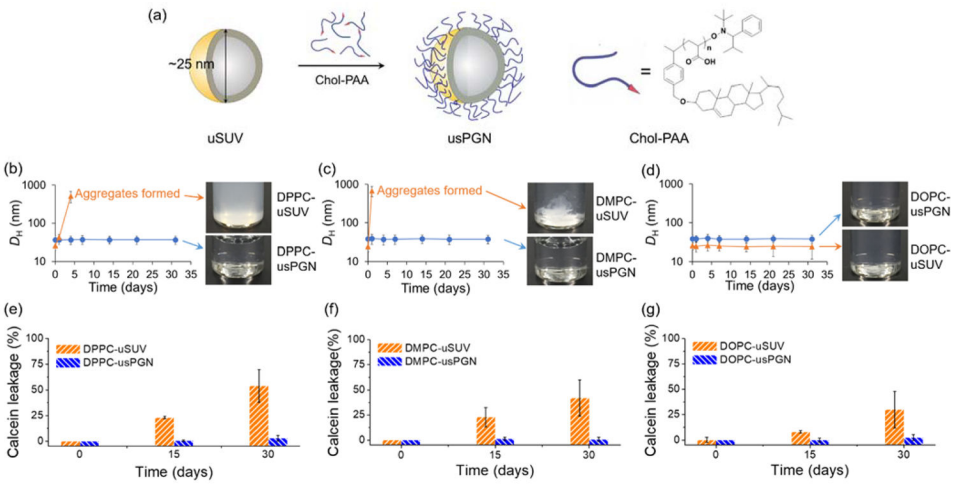

Figure 1.

Comparative stability and cargo-retention properties of uSUVs and usPGNs derived from DPPC, DMPC, and DOPC lipids. (a) Schematic illustration of usPGN preparation. (b–d) Hydrodynamic diameters (D_H) of uSUVs (orange triangle) and usPGNs (blue circle), as monitored by dynamic light scattering (DLS) over one month at 4 °C. The error bars represent the standard deviations from four different measurements. The inset pictures for DPPC- and DMPC-based formulations show clear differences between the uSUV and the usPGN materials: the former develop a cloudiness over time that is representative of aggregation. The aggregates can become so large in the case of DMPC that they eventually settle out of solution as can be seen in the wispy tendrils that were slightly stirred up in the inset picture for DMPC-uSUV in panel c. (e–g) The mean calcein leakage profiles up to 30 days at 4 °C for three batches of uSUVs (orange bar) and usPGNs (blue bar). The error bars represent the standard deviation of the mean calculated from three different batches.

Author Manuscript Author Manuscript Author Manuscript Author Manuscript

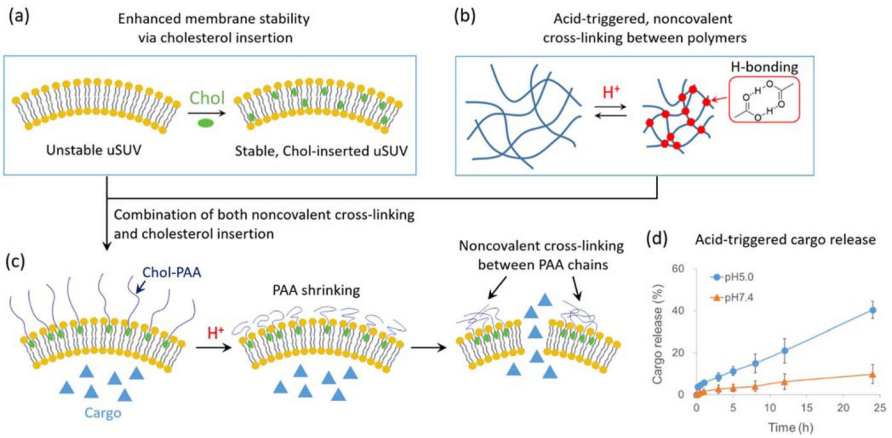

Figure 2.

Schematic illustration of the synergistic combination of cholesterol-induced membrane stability and pH-responsiveness in usPGN system. (a) The insertion of cholesterol moieties into the lipid bilayer membranes can increase the order of the lipid bilayer membrane[24,34] and stabilize defect sites,[19] thus reducing cargo leakage. (b) The formation of hydrogen bonds between carboxylic acid groups upon protonation leads to intra- and interchain noncovalent cross-linking of the polymer chains, causing clustering and shrinkage of the polymer mass. (c) The synergistic combination of cholesterol-induced membrane stability and noncovalent crosslinking results in the ability of usPGN to undergo acid-triggered cargo release. (d) Time-dependent cargo-releasing profiles of DOPC-usPGN$_{Rh}$ at pH 5.0 (blue circles) and pH 7.4 (orange triangles), respectively. The particles were incubated at 37 °C for 24 h, and the cargo (sulforhodamine B dye) released from the particles was quantified by fluorescence microscopy. Error bars represent the standard deviation of the mean calculated from three measurements.

Author Manuscript Author Manuscript Author Manuscript Author Manuscript

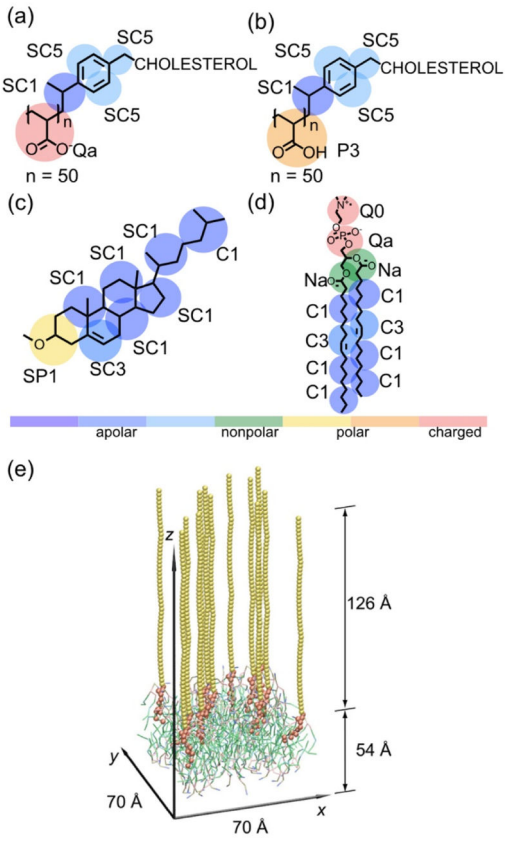

Figure 3.

(a–d) MARTINI mapping of coarse-grained beads for a Chol-PAA chain and DOPC lipid:[38] (a) 100% deprotonated and (b) 100% protonated Chol-PAA chains, (c) cholesterol anchor, and (d) DOPC lipid. The deprotonated and protonated AA monomers are represented as Qa (−1 charge) and P3 (0 charge) beads, respectively. Colored circles represent CG beads and each bead type is indicated in black next to the bead. (e) A snapshot of the initial setup for a DOPC lipid bilayer membrane model system with 10 mol % Chol-PAA grafts residing inside a simulation box comprising 0.15 M $NaCl_{aq}$, which mirrors the ionic media employed in the experiment. The embedded cholesterol anchors of the polymer chains are free to move on the membrane surface during the simulation with no positional restraints. Water and ions are omitted for clarity (see SI, Figure S8 for a detailed CG model system). The properties of the lipid bilayers such as bilayer thickness, area per lipid, and lipid order parameter can readily be obtained from simulations (SI, Table S9).

Author Manuscript Author Manuscript Author Manuscript Author Manuscript

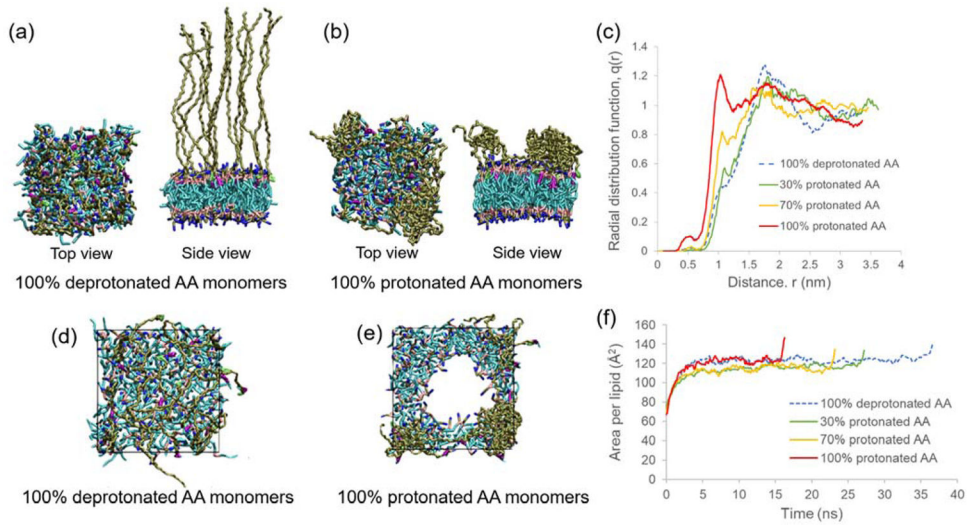

Figure 4.

(a and b) Top and side views of a Chol-PAA-grafted DOPC lipid bilayer membrane model with either 100% deprotonated AA repeating units (Qa/P3 = 100/0) (a) or 100% protonated AA repeating units (Qa/P3 = 0/100) (b) after 200 ns of CGMD simulation. The Chol-PAA chains with 100% deprotonated AA repeating units remain in extended conformations due to intra- and inter-chain electrostatic repulsion between the negatively charged Qa beads, while the chains with 100% protonated AA repeating units collapse onto the lipid membrane and form clusters. (c) The 2D (x–y plane) radial distributions of the cholesterol anchors for all four simulated DOPC lipid bilayers in our study (Qa/P3 = 100/0, 70/30, 30/70, and 0/100). These radial distribution profiles can be used to represent to the probability of finding one cholesterol molecule at a particular distance (r) from another one in the lipid bilayer, essentially correlating the “local” density of cholesterol to the overall “bulk” density. (d and e) Top views of a Chol-PAA-grafted DOPC lipid bilayer membrane model with either 100% deprotonated AA monomers (d) or 100% protonated AA monomers (e) after 20 ns of CGMD simulation at −45 bar of lateral pressure. The diameter of the pore in e is ~6 nm. All simulations were carried out in 10 × 10 nm^2 boxes, which were shown fully in the snapshots (a–b and d–e). For clarity, water and ions are omitted in these snapshots. (f) Plots of membrane area per lipid as a function of CGMD simulation time after the equilibrated lipid bilayer membranes were subjected to −45 bar of lateral pressure. The sharp increase in the membrane-area-per-lipid values at the end of simulations indicates membrane rupture, where the lipid dissociates from the surface.